Kinetics and Pathways of Charge Recombination in Photosystem II †

5 AUTHORS, INCLUDING:

Fabrice Rappaport
Institute of Physical and Chemical Biology
129 PUBLICATIONS **4,401** CITATIONS

SEE PROFILE

Mariana guergova Kuras
Ariana Pharmaceuticals
26 PUBLICATIONS **1,667** CITATIONS

SEE PROFILE

Peter J Nixon
Imperial College London
116 PUBLICATIONS **5,051** CITATIONS

SEE PROFILE

Kinetics and Pathways of Charge Recombination in Photosystem II[†]

Fabrice Rappaport,*,[‡] Mariana Guergova-Kuras,[‡] Peter J. Nixon,[#] Bruce A. Diner,[§] and Jérôme Lavergne[¶]

CNRS UPR 1261, Institut de Biologie Physico-Chimique, 13 rue Pierre et Marie Curie, 75005 Paris, France, and Department of Biochemistry, Imperial College, London, SW7 2AY, United Kingdom, and CR & D, Experimental Station, E. I. du Pont de Nemours & Co., Wilmington, Delaware, 19880-0173, USA, and CEA-Cadarache, DSV DEVM, Laboratoire de Bioénergétique Cellulaire (UMR163 CNRS CEA, Univ-Méditerranée CEA1000), 13108 Saint Paul-lez-Durance Cedex, France

ABSTRACT: The mechanism of charge recombination of the $S_2Q_A^-$ state in photosystem II was investigated by modifying the free energy gap between the quinone acceptor Q_A and the primary pheophytin acceptor Ph. This was done either by changing the midpoint potential of Ph (using mutants of the cyanobacterium *Synechocystis* with a modified hydrogen bond to this cofactor), or that of Q_A (using different inhibitors of the Q_B pocket). The results show that the recombination rate is dependent on the free energy gap between Ph and Q_A, which confirms that the indirect recombination pathway involving formation of Ph^- has a significant contribution. In the mutant with the largest free energy gap, direct electron transfer from Q_A^- to P^+ predominates. The temperature dependence of the recombination rate was investigated, showing a lower activation enthalpy in this mutant compared with the WT. The data allow the determination of the rate of the direct route and of its relative weight in the various strains. The set of currently accepted values for the midpoint potentials of the Q_A/Q_A^-, Ph/Ph^-, and P^+/P^* couples is not consistent with the relatively rapid rate of the indirect recombination pathway found here, nor with the 3% yield of delayed fluorescence as previously estimated by de Grooth and van Gorkom (1981, *Biochim. Biophys. Acta 635*, 445−456). It is argued that a likely explanation is that the midpoint potentials of the two latter couples are more positive than believed due to electrostatic interactions. If such is the case, the estimation of the midpoint potential of the P^+/P and S_2/S_1 couples must also be revised upward, with values of 1260 and 1020 mV, respectively.

The study of the recombination process occurring in photosynthetic reaction centers from the light-induced charge separated state has been a precious tool to investigate the electron transfer reactions and equilibria in the acceptor and donor chains of such systems. Several competing pathways are generally involved. Direct electron transfer may occur from the reduced terminal acceptor considered (e.g., the quinone acceptor Q_A^-) to the oxidized donor (e.g., the primary donor P^+). Indirect pathways may also occur where the electron passes through the primary pheophytin acceptor or even repopulates the excited state of the chlorophyll donor (P^*). The latter route has generally a small yield, but is important from an experimental standpoint, since it gives rise to delayed fluorescence emission.

The photochemical process in the reaction center of photosystem II of oxygenic photosynthesis is PPh → P*Ph → P^+Ph^-, where P[1] denotes the primary donor, and Ph is the primary acceptor (the pheophytin of the active branch on the D_1 polypeptide) (see ref *1* for a review). The formation of the singlet excited state P* generally occurs through excitation transfer from an antenna pigment. The transient radical pair (P^+Ph^-) may decay through electron transfer from Ph^- to P^+, or by reforming P* (followed by radiative or nonradiative exciton decay), but the most probable process is the stabilization of charge separation through the redox equilibria occurring on the acceptor side: $Ph^-Q_A ↔ PhQ_A^-$, and on the donor side: $S_1Y_ZP^+ ↔ S_1Y_Z^{ox}P ↔ S_2Y_ZP$. The S_2/S_1 couple denotes oxidation states of the Mn cluster involved in the storage of oxidizing equivalents in the water oxidase and Y_Z is the secondary donor (tyrosine D_1-161). Several routes for charge recombination can be considered: electron transfer from Q_A^- to P^+ or from Ph^- to P^+ (in these cases, the P^+/P couple is involved), or reformation of P* followed by exciton decay (the P^+/P^* couple is involved). Other routes, such as electron transfer from Ph^- to S_2 (Mn cluster) or Q_A^- to Y_Z^{ox}, can be disregarded due to the distances and equilibrium constants involved (see Discussion). We are thus considering three competing recombination processes, namely, the "direct" pathway involving electron transfer from Q_A^- to P^+, the "indirect" pathway

---

[1] Abbreviations: D1, the D1 polypeptide of the PSII reaction center; DCMU: diuron, 3-(3,4-dichlorophenyl)-1,1-dimethylurea; HEPES: *N*-(2-hydroxyethyl)piperazine-*N*′-(2-ethanesulfonic acid); P: the primary donor of photosystem II; Ph: pheophytin, primary electron acceptor in photosystem II; PSII: photosystem II; Q_A: primary quinone acceptor in photosystem II; Y_Z: D1-Tyr161, the redox active tyrosine of PSII on the D1 polypeptide.

Table 1: Estimations of the Midpoint Potentials in PS II[a]

(1)	(2)	(3)	(4)	(5)
Q_A/Q_A^-	Ph/Ph^-	P^+/P^*	P^+/P	S_2/S_1
-30 mV	-640 mV	-705 mV	1125 mV	885 mV
direct	direct	indirect	indirect	indirect

[a] The values in columns (1) and (2) were directly obtained from redox titrations. The other values all rely on (2) as explained below. (1) Data from refs *44* and *45*. (2) Data from refs *63*, *64*. (3) Based on (2) and the ΔG_0 of the exciton-radical pair equilibrium (45−80 mV, data from refs *79* and *80*) for PSII with normal antenna content). See also, for $D_1D_2b_{559}$ particles: (*81*, *82*) and for *Synechocystis* core particles: (*16*). (4) Deduced from (3) and the 1830 meV value of the singlet−singlet transition of P. (5) Deduced from (4) and assuming $\Delta G_0 = 240$ mV between P^+S_1 and PS_2 (representative of the range of estimations indicated in the text).

involving electron transfer from Ph^- to P^+ and the excitonic pathway. All three routes involve formation of P^+ through electron-transfer equilibrium with S_2. This scheme (leaving out the secondary donors) also applies to the reaction center of purple bacteria, where the recombination processes are better known than in PS II. The dominant pathway depends on the species. In *Rhodobacter sphaeroides* (*2*) or *Rhodobacter capsulatus* (*3*, *4*), direct transfer from Q_A^- (a ubiquinone molecule) to P^+ predominates, whereas in *Rhodopseudomonas viridis*, where Q_A is a menaquinone with a more negative midpoint potential, the indirect route through BPh^- predominates at room temperature (*5*). The direct route was found activationless (its rate is even accelerated at cryogenic temperatures), in contrast with the indirect route (see ref *6* for a review). The above pattern can be modified by substituting different quinones for Q_A (*2*, *7*). The key parameter is the free energy gap between BPh and Q_A: the thermally activated indirect route dominates when this gap is small enough, otherwise the direct, activationless path is favored.

In PS II, the relative weight of the indirect and direct pathways is not known. In his 1985 review, van Gorkom suggested that the indirect route was the major process at room temperature (*8*). Indeed, Reinman and Mathis found that $P^+Q_A^-$ charge recombination in Mn-depleted PSII, at pH 4 is thermally activated (*9*). In a recent thermoluminescence study, Vavilin and Vermaas brought qualitative evidence supporting a significant contribution of both the direct and indirect pathways in a temperature range close to or slightly lower than room temperature (*10*).

It should be realized, however, that currently accepted values of the redox couples involved in PS II (as compiled in Table 1) would predict a negligible contribution of the indirect route. The ΔE_m between Q_A and Ph would be about 600 mV, corresponding to an equilibrium constant of 10^{10} at room temperature. On the other hand, the electron-transfer rate from Ph^- to Q_A is around 3.3 ns^{-1} (*11*−*13*), so that the backward rate should be 0.33 s^{-1}. This rate constant provides an upper limit for the recombination through the indirect pathway. It is, however, more than 3 orders of magnitude smaller than the observed rate of recombination of $P^+Q_A^-$ (700−6000 s^{-1}, see ref *1*, for a review). This would seem to rule out completely the indirect pathway and to make the direct electron transfer from Q_A^- the only significant recombination route. Yet, there is at least one significant piece of evidence that does not agree with the figures of Table 1. The yield of the excitonic pathway was estimated

at about 3% by de Grooth and van Gorkom (*14*). From the values of Table 1, the equilibrium constant between Q_A^- and P^* should be 10^{11} ($\Delta E_m = 675$ mV) which would make delayed fluorescence an extremely weak phenomenon and markedly disagrees with the observed yield. The maximum rate of the excitonic pathway v_ϵ is k_ϵ/K_ϵ, where k_ϵ is the rate constant for exciton deactivation and K_ϵ is the overall equilibrium constant $[S_2PQ_A^-]/[S_1P^*Q_A]$. Since the observed recombination rate is about 0.2 s^{-1}, the finding of a 3% yield for the excitonic pathway implies $v_\epsilon \approx 6 \times 10^{-3}$ s^{-1}. With $k_\epsilon \approx 3 \times 10^8$ s^{-1} (*15*, *16*), one would obtain $K_\epsilon \leq 3 \times 10^8/6 \times 10^{-3} = 5 \times 10^{10}$, thus a maximum of 642 meV for the free energy difference between the exciton and the stabilized $S_2Q_A^-$ state. This is less than the energy difference given by Table 1 between the exciton and the state $P^+Q_A^-$ and would just leave no room for the stabilization occurring on the donor side between P and the S system. A similar analysis was previously developed by van Gorkom (*8*) who concluded that the energy gaps on the acceptor side were smaller than generally believed, with a ΔE_m between Q_A and Phe of about 340 mV that would make the indirect route the major recombination pathway.

The data reported in the present work show that the indirect pathway is indeed the major route for recombination in PS II, in clear disagreement with the E_m estimations of Table 1. We have compared the recombination kinetics in the wild type and in two mutants of the cyanobacterium *Synechocystis* sp. PCC 6803. The mutants bear a substitution of the glutamine D_1-130 to either glutamate (Q130E strain) or leucine (Q130L) to modify the strength of the hydrogen bond between this residue and Ph. As previously shown (*17*−*19*), these substitutions result in modifications of the midpoint potential of the Ph/Ph^- couple in a similar way as achieved for the bacterial P by Allen and co-workers (*20*) (these authors engineered mutant strains of *R. sphaeroides* which presented important shifts of the midpoint potential of the primary donor due to the addition or removal of hydrogen bonds to P). As illustrated below, the recombination rate of PS II is modified in the Q130 mutants, demonstrating the involvement of the indirect pathway. This finding leads to a significant revision of the E_m values shown in Table 1. This revision is of particular consequence, since the only values that were directly measured from equilibrium redox titrations are those of Q_A and Ph, while the others, including those pertaining to the donor side, are positioned with respect to these at distances estimated from the various equilibrium constants.

MATERIAL AND METHODS

All the *Synechocystis* 6803 strains used here are derivatives of the glucose-tolerant strain described in ref *21*. The control strain, referred to here as WT, is strain TC35, a deletion mutant containing just one (*psbA3*) of the three members of the *psbA* gene family. Mutants D1-Q130E and D1-Q130L were constructed as described in ref *22* and have been used in previous studies (*17*, *18*). The cyanobacteria were grown in glucose-free BG11 medium under dim light. Cells were harvested by centrifugation at 3000*g* for 5 min and resuspended in fresh BG11 medium to which 0.3 mM *p*-benzoquinone, 0.3 mM ferricyanide, and 50 mM Hepes pH 7.2 was added. The optical density at 730 nm was 0.8. DCMU or bromoxynil were added to inhibit the electron

transfer from Q_A^- to Q_B, at concentrations of 10 and 30 μM, respectively, that were checked to be saturating. To measure the $S_2Q_A^-$ decay, a single flash was given to whole cells, and the rate of relaxation of the chlorophyll fluorescence yield was examined. Fluorescence was measured with a home-built spectrophotometer described in ref 23. The actinic flash was a xenon flash lamp (2 μs at half-height) with a broad band blue filter. The fluorescence emission was excited by discrete weak monochromatic flashes (450 nm) and detected through a combination of filters rejecting wavelengths < 650 nm. Experiments at variable temperature were done in a similar way, using the setup described by Joliot et al. (24).

To estimate the distortion caused by the nonlinear dependence of the fluorescence yield with respect to $[Q_A^-]$ (25, 26), we compared the kinetics induced by a saturating flash and by a weak flash hitting 15% of the centers (not shown). In the latter case, the distortion is expected to be negligible. The "true" recombination kinetics thus obtained is about 3.4-fold slower than that observed after a saturating flash (based on the ratio of the half-times), and the plot of the saturating vs weak flash kinetics gives a hyperbolic dependence with $p \approx 0.74$ for Joliot's connection parameter (25). With respect to this parameter some variability was observed, probably due to an unknown parameter in culture conditions. However, the half-times found after correction were similar. The finding of a pronounced hyperbolic dependence in this material is at variance with ref 22 but was previously observed in cyanobacteria (27). The recombination kinetics observed when using either the weak flash or saturating flash had multiple components and could be fitted by a sum of two exponentials. Such a heterogeneous decay of $S_2Q_A^-$ appears to be the rule in PS II (28) and was also observed for $P^+Q_A^-$ recombination (29, 30). It may be noted that by itself, the hyperbolic distortion would transform a single decay exponential into nonexponential fluorescence kinetics. The fluorescence kinetics after the saturating flash happened to be well fitted by a sum of two exponentials (Figure 1), but this is mainly coincidental and bears no simple relationship with the components of the recombination kinetics. This decomposition was only used to check that the mutants had a similar kinetic heterogeneity as the WT (i.e., both apparent phases were slowed or accelerated to similar extent and their relative amplitude remained similar). To quantify the recombination rate, we used the overall half-time of the fluorescence decay in the expression $v_{rec} = \ln(2)/(3.4t_{1/2})$, where the factor 3.4 accounts for the acceleration of the fluorescence decay (saturating flash) with respect to the recombination kinetics (weak flash).

RESULTS

According to resonance Raman measurements (31) and predicted folding or structural models (32–34), the residue present at position 130 of polypeptide D_1 lies in the vicinity of pheophytin A and could provide a hydrogen bond to the C9-keto group of this cofactor. The role of this residue was investigated by site-directed mutagenesis in which the glutamine was replaced by a glutamic acid (Q130E) or a leucine (Q130L). The Q130E mutation is particularly conservative as a glutamic acid occupies this position in higher plants and the photosynthetic purple bacteria. The consequences of the Glu to Leu, or Glu to Gln substitutions on
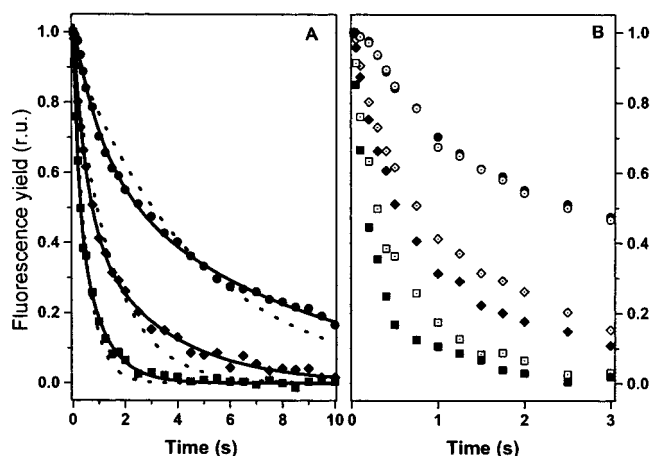

FIGURE 1: (A) Decay of the fluorescence yield decay after a saturating flash in the presence of DCMU in whole cells of *Synechocystis* 6803 WT (diamonds), Q130E (squares), and Q130L (circles). The overall lifetimes (i.e., ln $2/t_{1/2}$) are 300 ms, 700 ms, and 2s for the Q130E, WT, and Q130L, respectively. The solid lines are the best fits with a sum of two exponentials (half times: Q130E: 110 ms (55%), 600 ms (45%), WT: 300 ms (50%), 1.7 s (50%), and Q130L: 850 ms (50%), 5.2 s (50%)). (B) The decay kinetics observed in the presence of DCMU (open symbols) or bromoxynil (solid symbols).

the BPh^-/BPh FTIR spectrum have been investigated in *R. sphaeroides* and *R. viridis* reaction centers (35, 36). These studies show that the hydrogen bond to the 9-keto group of the bacterio pheophytin is weakened or suppressed when Glu is replaced by Gln or Leu, respectively, and that the Leu mutation results in a structural modification evidenced by a frequency shift of the 10a-ester group of the pheophytin. In PSII, a hydrogen bond between the pheophytin ring and the Glu130 has been recently evidenced by high-field EPR. According to these studies, the strength of this hydrogen bond is decreased when the glutamic acid is replaced by a glutamine and further weakened when changed for a leucine (19). As expected, the mutations affect the midpoint potential of the pheophytin. This was shown by Merry et al. (18) who found that that the free energy stored in the radical pair after charge separation in PS II reaction centers purified from Q130E and Q130L was smaller or larger, respectively, than in the wild type. In this manner, the authors estimated that the E_m of the pheophytin couple was shifted by +33 mV in Q130E and by −74 mV in Q130L with respect to the WT. This agrees with a previous study of the same group reporting modifications of the quantum yield of primary charge separation (decreased in Q130L and increased in Q130E with respect to WT) (17). Consequently, these mutations are expected to change the difference in free energy between the PhQ_A^- and the Ph^-Q_A states and thus the probability to repopulate the P^+Ph^- state from the $P^+Q_A^-$ state. The comparison of the recombination kinetics in the WT, the Q130E, and the Q130L strains provides a tool to study the contribution of the thermally activated repopulation of the P^+Ph^- state to this process.

Figure 1A shows the decay of the fluorescence yield after a single saturating flash in the presence of DCMU, in the WT (diamonds), the Q130E (squares), and the Q130L (circles) strains. The kinetics may be fitted by a sum of two exponentials (see legend), but this decomposition bears little significance because of the distortion caused by the hyperbolic dependence of the fluorescence yield on the amount
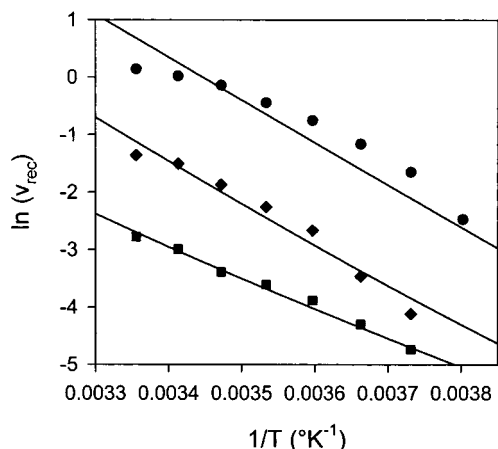
FIGURE 2: Arrhenius plots $\ln(v_{rec})$ vs $1/T$ for the recombination kinetics in the presence of DCMU for the three strains: Q130E, circles; WT, diamonds; Q130L, squares. The lines are theoretical plots obtained with G_{SP} ($T = 293$ K) = 233 meV ($\Delta H = 53$ meV, $\Delta S = 0.61$ meV K^{-1}), G_{QPh} ($T = 293$ K) = 345 meV ($\Delta H = 285$ meV, $\Delta S = -0.20$ meV K^{-1}). The shifts of E_m(Ph) with respect to the WT are -74 mV and $+35$ mV for Q130L and Q130E, respectively. Other parameters as derived in the text ($k_{QP} = 410$ s^{-1}, $k'_{PhP} = 1.6 \times 10^9$ s^{-1}).

of closed centers (see Methods). To characterize the recombination rate, we have used the quantity $v_{rec} = \ln(2)/(3.4t_{1/2})$, where $t_{1/2}$ is the overall half-time of the fluorescence decay and the factor 3.4 is the correction for the apparent acceleration caused by the hyperbolic distortion. As shown in Figure 1A, the Q130E substitution results in an increased rate with respect to the control strain TC35 by a factor of about 4, while the Q130L substitution slows down the recombination by about the same factor. Thus, it appears that the recombination rate is sensitive to the E_m of Ph, demonstrating a significant contribution of the indirect pathway. At 20 °C, we obtained $v_{rec} \approx 0.22$ s^{-1} for the WT, 1.02 s^{-1} for Q130E, and 0.05 s^{-1} for Q130L (in spinach PS II, one has $v_{rec} \approx 0.2$ s^{-1}).
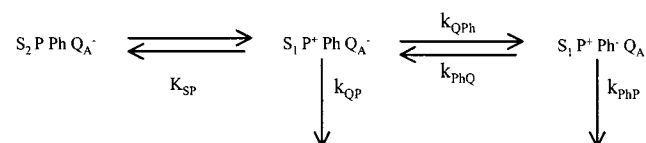
Another way to modify the ΔE_m of the Ph$^-$ Q$_A$ $\leftrightarrow$ Ph Q$_A^-$ equilibrium is to change the E_m of the Q$_A$/Q$_A^-$ couple. Krieger-Liszkay and Rutherford (*37*) reported that the redox potential of this couple is more negative in the presence of phenolic inhibitors of the Q$_B$ pocket such as bromoxynil than in the presence of a phenyl urea inhibitor such as DCMU. Figure 1B shows the fluorescence yield decay in the WT, Q130E, and Q130L strains, in the presence of DCMU (open symbols) and bromoxynil (closed symbols). Both in Q130E and WT the decay was faster when using bromoxynil, by factors of about 1.75 and 1.5, respectively. In the Q130L strain, however, the decay was not sensitive, within experimental accuracy, to the nature of the inhibitor. The acceleration caused by bromoxynil in the WT and in Q130E is again consistent with a significant contribution of the indirect pathway, which is favored when the ΔE_m between Ph and Q$_A$ is smaller.

To determine the activation enthalpies involved in the recombination process, we measured the temperature dependence of the S$_2$Q$_A^-$ lifetime. The plots of $\ln(v_{rec})$ as a function of $1/T$ are presented in Figure 2. The temperature range is restricted to the region -5 to 25 °C because we observed irreversible (or very slowly reversible) modifications of the kinetics when cooling below -5 °C or heating

above 25 °C. This problem was not remedied when suspending the cells in a glycerol/water mixture. In the three strains, the rate of charge recombination significantly decreased when lowering the temperature. The plots are approximately linear for the WT and Q130 L, with activation enthalpy of 610 and 450 meV, respectively.

DISCUSSION

Direct vs Indirect Recombination Pathways. The present results show that the recombination rate of state S$_2$Q$_A^-$ is sensitive to the free energy gap between Ph and Q$_A$. When this gap is decreased or increased, either by changing the E_m of Ph (by substitution of the Q130 residue) or that of Q$_A$ (by changing the inhibitor), the rate is accelerated or slowed, respectively. A straightforward conclusion is that the indirect pathway, passing via the P$^+$Ph$^-$ state represents a significant contribution to the overall process. The sensitivity to the nature of the inhibitor is lost, however, in the Q130L mutant, suggesting that in this mutant, the indirect pathway has been slowed to such an extent that the direct pathway has become predominant. Accordingly, the recombination rate in this mutant can be taken as a good approximation for the rate v_{dir} of the direct pathway (we denote by v the effective rate constants pertaining to the decay of state S$_2$Q$_A^-$, using k in other cases). In this manner, one obtains $v_{dir} = 0.05$ s^{-1}. On the other hand, the recombination rate in the WT is $v_{rec} = 0.22$ s^{-1}. Since $v_{rec} = v_{dir} + v_{ind}$ (where v_{ind} stands for the rate of the indirect pathway and neglecting the excitonic pathway), one deduces $v_{ind} = 0.17$ s^{-1}. Thus, in the WT, the indirect pathway is predominant and accounts for $0.17/0.22 = 77\%$ of the overall process. We will now discuss the information that can be derived from these data concerning the E_m changes of the Ph/Ph$^-$ couple in the mutants with respect to WT and compare this with the estimations obtained by Merry et al. (*18*). We consider the kinetic scheme:

$$S_2 P\, Ph\, Q_A^- \underset{K_{SP}}{\overset{}{\rightleftharpoons}} S_1 P^+ Ph\, Q_A^- \quad\underset{k_{QP}}{\big\downarrow} \overset{k_{QPh}}{\underset{k_{PhQ}}{\rightleftharpoons}} S_1 P^+ Ph^-\, Q_A \quad\underset{k_{PhP}}{\big\downarrow}$$

where the indicated rate constants are k_{QP} and k_{PhP} for recombination from Q$_A^-$ and Ph$^-$, respectively, k_{PhQ} and k_{QPh} are for electron transfer between Q$_A$ and Ph, and K_{SP} is the equilibrium constant [S$_2$P]/[S$_1$P$^+$]. We assume that the latter equilibrium is rapid with respect to recombination (this assumption is supported by the very rapid recombination rate observed in electroluminescence experiments despite the moderate electrogenicity between S$_2$ and P (see ref *14*)). This implies

$$v_{dir} = \frac{k_{QP}}{K_{SP}} \tag{1}$$

As will be verified later, the approximation based on a rapid equilibrium on the acceptor side is not valid, and we use the more accurate expression (see Figure 3 for a recombination scheme in PSII):

$$v_{ind} = \frac{1}{K_{SP}} \frac{k_{QPh}k_{PhP}}{k_{PhP} + k_{PhQ}} = \frac{1}{K_{SP}K_{QPh}} \frac{k_{PhQ}k_{PhP}}{k_{PhP} + k_{PhQ}} \tag{2}$$
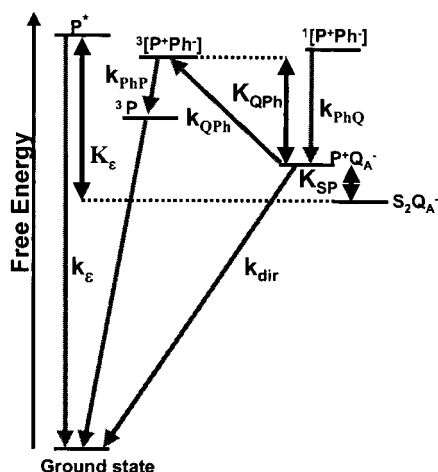
FIGURE 3: Recombination scheme in PS II, indicating the rate (ks and gray arrows) and equilibrium (Ks and black double arrows) constants featuring in Table 3.

where $K_{QPH} = k_{PhQ}/k_{QPh}$. The rationale for eq 2 is that whenever state $S_1P^+Ph^-Q_A$ is formed, it has a probability $k_{PhP}/(k_{PhP} + k_{PhQ})$ to recombine. It may be seen that this expression agrees with the rapid equilibrium approximation when $k_{PhQ} \gg k_{PhP}$ and conversely expresses the rate limitation by k_{QPh} when $k_{PhQ} \ll k_{PhP}$. Equation 2 may be rewritten:

$$v_{ind} = \frac{k'_{PhP}}{K_{SPh}} \qquad (3)$$

where $K_{SPh} = K_{SP}K_{QPh}$ is the overall equilibrium constant $[S_2PPhQ_A^-]/[S_1P^+Ph^-Q_A]$ and k'_{PhP} is the rightmost term in eq 2. One has, at a temperature around 300 °K:

$$60\log K_{SPh} = E_m^P - E_m^S + E_m^Q - E_m^{Ph} \qquad (4)$$

where the E_m's are the midpoint potentials of the various couples expressed in mV. For a mutant where E_m^{Ph} is shifted by ΔE_m^{Ph} with respect to the WT,

$$v_{ind}(\Delta E_m^{Ph}) = v_{ind}(0)10^{\Delta E_m^{Ph}/60} \qquad (5)$$

(assuming that the rate constants k_{PhQ} and k_{PhP} are not significantly modified). The overall recombination rate is then:

$$v_{rec}(\Delta E_m^{Ph}) = v_{dir} + v_{ind}(0)10^{\Delta E_m^{Ph}/60} \qquad (6)$$

The solid line in Figure 4 shows a plot of $\ln(v_{rec})$, assuming $v_{dir} = 0.05$ s^{-1} (the recombination rate of Q130L) and $v_{ind}(0) = 0.17$ s^{-1} (so that $v_{rec}(0) = 0.22$ s^{-1} as found for the WT). The solid horizontal lines indicate $\ln(v_{rec})$ for each strain. One can thus estimate $\Delta E_m^{Ph} \approx +48$ mV for Q130E and $\Delta E_m^{Ph} \le -90$ mV for Q130L. These shifts are somewhat larger than found by Merry et al.; ($+33$ and -74 mV, respectively), indicated by the vertical lines. On the other hand, if we combine Merry's estimates for the ΔE_m^{Ph} and our recombination rates (symbols) and search for the best fit using eq 6, we obtain $v_{dir} = 0.04$ s^{-1} and $v_{ind}(0) = 0.23$ s^{-1} (dashed curve in Figure 4). This would imply that the recombination process in Q130L still involves a 20% ($1 - 0.04/0.05$) contribution of the indirect pathway and that the acceleration caused by bromoxynil was below our experi-
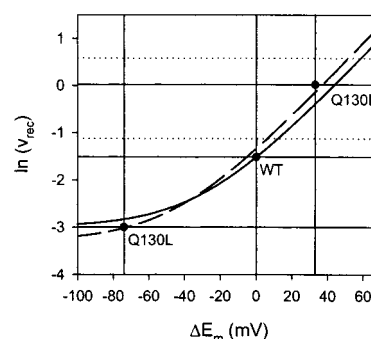

FIGURE 4: A plot of $\ln(v_{rec})$ for the three strains (with DCMU, solid horizontal lines, or with bromoxynil, dotted horizontal lines) vs the shift of E_m(Ph) with respect to the WT. The solid vertical lines indicate the ΔE_m values determined by Merry et al. for Q130L and Q130E. The solid curve is the theoretical prediction (for the DCMU data) assuming $v_{dir} = 0.05$ s^{-1} (Q130L value) and $v_{ind} = 0.17$ s^{-1} (WT value − Q130L value). The dashed curve is the best fit (for the DCMU data) with v_{dir} and v_{ind} as free parameters (the fit values are 0.04 and 0.23 s^{-1}, respectively).

mental resolution. The dotted horizontal lines in Figure 3 show the recombination rates measured in the presence of bromoxynil for WT and Q130E. The ΔE_m^Q caused by this inhibitor with respect to DCMU can be estimated at about -14 mV, much smaller than determined in spinach PS II (-90 mV) by Krieger et al. (*37*).

Donor Side Equilibrium and Direct Recombination Rate. Relevant literature data about K_{SP} can be summarized as follows. The equilibrium constant for electron transfer between P and Y_Z has been estimated in the 5−29 range (*38−40*) during the transient equilibrium reached in the microsecond range following a flash. This would imply a 40−90 meV energy gap. From electroluminescence measurements, Vos et al. (*41*) estimated a 55 meV difference between S_2/S_1 and Y_Z^{ox}/Y_Z. Adding these values gives $G_{SP} = 95$−145 meV. Both measurements, however, are obtained at short times and the relevant value for G_{SP} may include additional stabilization occurring on a longer time-scale. Another estimation uses the ratio of recombination rates of $P^+Q_A^-$ and of $S_2Q_A^-$. In Mn depleted material, with Y_Z oxidized prior to the flash, the $P^+Q_A^-$ recombination proceeds with a rate constant of 6000 s^{-1} (in spinach thylakoids, *29*) or 4100 s^{-1} (in *Synechococcus*, *42*) based in both cases on the major fast phase of the multiphasic decay. In a mutant of *Synechocystis* with Y_Z deleted, Metz et al. (*43*) measured a rate of 700 s^{-1}. The recombination rate of $S_2Q_A^-$ in spinach is about 0.2 s^{-1}. This would imply $K_{SP} = 3 \times 10^4 - 3.5 \times 10^3$, or $G_{SP} = 200$−260 meV. A complication arises from the finding (*44, 45*) that the midpoint potential of Q_A is shifted up by about 150 mV in Mn-depleted material where the $P^+Q_A^-$ recombination was measured. According to the present study, this effect should markedly slow the recombination, probably switching from the indirect-dominant to direct-dominant regime (as observed here when comparing the Q130E and Q130L strains). This would imply, roughly, a 20-fold slowing, meaning that the $P^+Q_A^-$ recombination rate is in the range $12 \times 10^4 - 14 \times 10^3$ s^{-1} in O$_2$-evolving PSII, i.e., $G_{SP} = 290$−350 meV.

It thus appears that the uncertainty on G_{SP} is very large. We can, however, obtain an independent estimate by comparing our value of $v_{dir} \approx 0.05$ s^{-1} with the value of k_{PQ} determined at low temperature. A rate of 410 s^{-1} ($t_{1/2} \approx 1.7$

Table 2

Estimations from the literature:

Rate constants: $k_\varepsilon = 3 \cdot 10^8$ s^{-1} (*15;16*), $k_{PhP} = 3 \cdot 10^9$ s^{-1} (*48*), $k_{PhQ} = 3.3 \cdot 10^9$ s^{-1} (*11;13*), $k_{QP} = 410$ s^{-1} (*9;30*).

Yield of the excitonic recombination pathway: $\eta = 0.028$ (*14*).

Rate constants for S₂Q$_A^-$ recombination (this paper):

$v_{rec} = 0.22$ s^{-1}, $v_{dir} = 0.05$ s^{-1}, $v_{ind} = 0.17$ s^{-1}.

Equations and numerical values derived in the text:

$$K_{SP} = \frac{k_{QP}}{v_{dir}} \approx 10^4 \quad (G_{SP} \approx 240 \text{ meV})$$

$$v_{ind} = \frac{k'_{PhP}}{K_{SP}K_{QPh}} \quad \text{with } k'_{PhP} = \frac{k_{PhQ}k_{PhP}}{k_{PhQ} + k_{PhP}} = 1.6 \cdot 10^9 \text{ s}^{-1}$$

$$K_{QPh} = \frac{k'_{PhP}}{v_{ind}K_{SP}} \approx 10^6 \quad (G_{QPh} \approx 360 \text{ meV})$$

$$K_\varepsilon = \frac{k_\varepsilon}{\eta v_{rec}} \approx 5 \cdot 10^{10} \quad (G_\varepsilon \approx 640 \text{ mV})$$

---

ms) was reported by several groups (*9, 30*) for P$^+$Q$_A^-$ recombination at cryogenic temperatures. This rate constant clearly pertains to the direct pathway (because of the high activation energy implied by the indirect route). It is in very good agreement with the empirical expression derived from Marcus theory by Moser and co-workers (*46*), stating that for an activationless reaction:

$$\log(k) = 15 - 0.6R \quad (7)$$

where R is the edge to edge distance in Angstroms. From the crystallographic data (Table 2), one has $R = 20.4$ Å between P and Q$_A$, which would predict $k_{PQ} \approx 575$ s^{-1} (applying the standard deviation estimated by Moser and co-workers, the range is $240-1380$ s^{-1}). It is unlikely that this maximum rate could be significantly accelerated at room temperature (in bacteria, the homologous reaction is actually slower at room temperature by a factor $3-4$ compared with low temperature). It we assume that it is essentially temperature independent, then $k_{PQ} \approx 410$ s^{-1} and $K_{SP} \approx k_{PQ}/v_{dir} \approx 10^4$. We will thus adopt $G_{SP} = 240$ meV as a reasonable value. This is in good agreement with the estimations derived from the overall recombination rates of S₂Q$_A^-$ and P$^+$Q$_A^-$, provided that the correction accounting for the E_m shift of Q$_A$ in Mn-depleted material is ignored. A possible explanation is that the disruption of the Mn cluster affects in a similar

way both Q$_A$ and Ph, so that the ΔE_m between them is little modified.

The recombination rate of P$^+$Q$_A^-$ (direct + indirect routes) can then be estimated to be $v_{rec}K_{SP} \approx 0.22 \times 10^4 = 2200$ s^{-1}, which is in reasonable agreement with the values ($4000-6000$ s^{-1}) measured in Mn-depleted material in the presence of Y$_Z^{ox}$ (notice that these figures represent the fast phase of the multiphasic recombination).

Equilibrium Constants on the Acceptor Side and Indirect Recombination Rate. We have obtained $v_{ind} \approx 0.17$ s^{-1} in the WT. From this value and literature data concerning k'_{PhP} (see eqs $2-3$), we will now estimate the equilibrium constant K_{SPh}. Our working scheme is indicated in Figure 3, while Table 2 summarizes the numerical values and equations. Depending on the spin correlation, the radical pair P$^+$Ph$^-$ can be found in a singlet or triplet state. The magnetic interaction between the unpaired electrons residing on P$^+$ and Ph$^-$ is negligible, so that the singlet and triplet states should be isoenergetic (same enthalpy). The triplet state has, however, a 3-fold degeneracy, which implies that its entropy is larger than that of the singlet by $k_B\ln(3)$ (where k_B is the Boltzmann constant), corresponding to a lower free energy by about 30 mV (at room temperature) (*8*). When formed from P*, the radical pair is initially entirely in the singlet state and, if electron transfer to Q$_A$ is prevented, the singlet–

triplet equilibration occurs in the 5−50 ns time range (*47*). On the other hand, when the radical pair is formed from a stabilized state (e.g., $P^+Q_A^-$), the spin equilibrium is present from the start. The rate constant of the decay of the triplet state, forming triplet P (^3P), has been estimated at about 3 ns^{-1} at 290 K (*48*). Altogether, these figures are consistent with the rate of 0.05 ns^{-1} found for the decay of P^+Ph^- (accompanied by formation of ^3P) when formed in the light in the presence of the quinol form of Q_A (so that electron transfer is prevented while keeping an electrically neutral form of Q_A) (*49*). The rate-limiting process appears to be the spin dephasing, while the triplet electron-transfer reaction $^3[P^+Ph^-] \rightarrow {}^3P$ is the fastest and major pathway for the radical pair decay. The 3 ns^{-1} rate constant for this process turns out to be similar to that of the Ph$^-$ to Q_A electron transfer. Clearly, the $^1[P^+Ph^-] \rightarrow {}^1P$ recombination process must be much slower than that if a good quantum yield of the charge stabilized state is desired. As suggested by van Gorkom (*8*), the exciton-radical pair equilibrium, together with the nonexponential (null initial rate) of the singlet−triplet conversion are likely to minimize losses through the triplet pathway during the charge separation process. On the basis of the above considerations, we assume that this route, with rate constant ≈ 3 ns^{-1}, is the major decay process for the radical pair P^+Ph^- and neglect the decay from the singlet state (thus, $k_{PhP} \approx 3$ ns^{-1}). Notice that the forward rate k_{PhQ} must be the same for the triplet and singlet states of the radical pair. The degeneracy of the triplet affects the backward rate (3-fold larger than for the singlet) and is appropriately taken into account in the above equation, provided k_{QPh} and K_{QPh} refer to the triplet state.

With $k_{PhQ} = 3.3 \times 10^9$ s^{-1}, $k_{PhP} = 3 \times 10^9$ s^{-1}, one obtains for k'_{PhP} (defined in eqs 2−3): $k'_{PhP} = k_{PhQ}k_{PhP}/(k_{PhP} + k_{PhQ}) = 1.6 10^9$ s^{-1} and therefore $K_{SPh} = k'_{PhP}/v_{ind} \approx 10^{10}$, corresponding to a free energy difference of about 600 meV between states $S_2PPhQ_A^-$ and $^3(S1P^+Ph^-Q_A)$. This is close to the enthalpy difference deduced from the temperature dependence of the recombination rate of the WT (or of spinach PS II, see below).

We obtained above (see introduction), using de Grooth's estimation of the yield of the exciton pathway, a figure of 640 meV for the free energy gap between $S_2Q_A^-$ and the exciton. If one assumes that P* is isoenergetic with an antenna of 200 chlorophylls, this implies an entropic stabilization of 140 meV due to exciton dilution over the antenna (or 100 mV in PSII core complexes with 40 chlorophylls). The free energy level difference between P* and the $S_2 Q_A^-$ state is then about 780 meV. For the energy difference between P* and the triplet radical pair, we have thus 780−600 = 180 meV, or 150 meV between P* and the singlet radical pair. This is close to the 135 meV estimated by Booth et al. from luminescence measurements in the 100 ns time range using $D_1D_2b_{559}$ reaction centers (*50*) and suggests that there is no major relaxation process that would further stabilize P^+Ph^- when formed during the recombination of $S_2Q_A^-$.

The free energy difference G_{QPh} between Q_A and Ph is (600 meV − G_{SP}). Therefore, if $G_{SP} \approx 240$ meV, then $G_{QPh} \approx 360$ meV. This implies that the 610 meV value of Table 1 is overestimated by about 250 meV.

Other Recombination Routes. We have only considered thus far the recombination routes involving electron transfer

Table 3: Edge-to-Edge and Center-to-Center Distances in PS II, from the PDB Coordinates of 1FE1 (*38*)[a]

	P	Ph	Q_A
Mn (S_2)		**24.6**	**38.6**
Y_Z		**18.5**	**33.0**
P		**8.3**	**20.4**
Ph	*15.5* (P$_A$)		
	19.5 (P$_B$)		
Q_A		*11.1*	

[a] Bold: edge to edge distance, italic: center to center. P$_A$ and P$_B$ are the chlorophylls of the special pair on the A (D1) and B (D2) branches, respectively.

to P^+ and disregarded other possibilities, such as electron transfer to Mn (S_2) or Y_Z^{ox} (from Ph$^-$ or Q_A^-). Upper limits for the relative weights of these pathways can be obtained by combining the available information on equilibrium constants and distances. Using eq 7 and the distance data of Table 3 (from ref *51*), one obtains 2×10^{-5} s^{-1} for $Y_Z^{ox}Q_A^- \rightarrow Y_ZQ_A$ (i), 2 s^{-1} for $S_2Ph^- \rightarrow S_1Ph$ (ii) and 8000 s^{-1} for $Y_Z^{ox}Ph^- \rightarrow Y_ZPh$ (iii). Process (i) is obviously negligible. The other ones can be discarded, too, by considering the equilibrium constants involved to form these states. Assuming that $k_{PhP} \approx 3 \times 10^9$ s^{-1}, then process (ii) could be competitive only if S_2 were about 10^9 times more populated than P^+, in contrast with the equilibrium constant of 10^4 estimated above. Similarly, process (iii) could be competitive if Y_Z^{ox} were about 4×10^5 times more populated than P^+, again larger than the overall equilibrium constant between S_2 and P. Thus, all these possibilities can be neglected—with, however, a smaller margin for case (iii).

Temperature Dependence. The Arrhenius plots shown in Figure 2 yield estimations of the activation enthalpy for the recombination reaction: $H_{ac} \approx 610$ meV for the wild type and ≈ 450 meV for the Q130L mutant. The plot obtained for Q130E is not linear, with a smaller slope in the high temperature region (a similar but less pronounced trend is also observed for the wild type). Due to this problem and because of the restricted temperature range that the cells could withstand, quantitative analysis of the data is limited. Nevertheless, there is clearly a decrease of the activation enthalpy in the Q130L mutant with respect to WT. This is good qualitative evidence that the recombination process switches from a regime where the indirect pathway is significant (WT) to one dominated by the direct pathway (Q130L). Indeed, when the ΔE_m between Q_A and Ph is increased, the contribution of the indirect pathway must undergo both a decrease of its rate *and* an increase of its activation enthalpy, while this does not affect the contribution of the direct pathway (which is expected to have a smaller activation enthalpy). Thus, this observation confirms our interpretation of the bromoxynil/DCMU experiment. The activation enthalpy found for the WT (610 meV) is somewhat larger than that measured by Kanazawa and Kramer in spinach thylakoids (578 meV), which could be expected since plant PS II has a glutamate at position 130, thus equivalent to Q130E (this equivalence must be qualified, however, because the recombination rate of chloroplast PS II is closer to that of the cyanobacterial WT than to Q130E). A much larger activation enthalpy was estimated from thermoluminescence data (≈ 810 meV) (*52*). It should be noted, however, that the theoretical framework used for such

estimations, either using the Randall-Wilkins equation (*53*) or the more elaborate treatment developed by Devault and co-workers (*54*) all assume that the excitonic pathway is the only decay process for $S_2Q_A^-$, which is obviously inappropriate. The recent study of Vavilin (*10*) showing drastic changes of the thermoluminescence peak temperature and intensity in mutants where the E_m of P is modified gives a clear illustration of this point.

According to the present interpretation, the activation enthalpy for Q130L ($\approx$ 445 meV) should reflect essentially the ΔH between the S_2/S_1 and P^+/P couples. If such is the case, and if G_{SP} is 240 meV, the entropy of the S_2P state must be significantly lower than that of S_1P^+ ($T\Delta S \approx 200$ meV). On the other hand, the activation enthalpy for the indirect pathway (about 610 meV in the WT, or 578 meV in spinach PS II) is similar to our estimate of $G_{SPh} \approx 600$ meV, which suggests that the overall entropy difference between states $S_2Q_A^-$ and P^+Ph^- is small. This implies that entropy contribution to G_{SP} would be partly canceled out by a contribution of opposite sign in G_{QPh} ($T\Delta S \approx -60$ meV at room temperature, according to the fit shown in Figure 2). The finding by Reinman and Mathis or van Gorkom et al. (*9*, *55*) of $\Delta H_{QPh} \approx 160$ meV (from the activation enthalpy of the recombination of $P^+Q_A^-$ in spinach PS II) also suggests a significant negative ΔS at this step (i.e., one would have in this case $G_{QPh} \approx 360$ meV with $\Delta H = 160$ meV and $T\Delta S = -200$ meV).

A Revision of the E_m Picture. We have argued that the currently accepted E_m values compiled in Table 1 cannot account for the recombination data. The ΔE_m between the (Q_A/Q_A^-) and (Ph^-/Ph) or (P^+/P^*) couples must be smaller by about 250 mV. Only two of the E_m values featured in the table have been directly measured from redox titrations, that of Q_A and that of Ph. The question is then, which is the "wrong" one: is it Q_A (that should be located around -300 mV rather than -30 mV) or Ph (that should be located around -390 mV rather than -640 mV)? It may be noted that both sets of data pertain to rather slow time scales (the seconds range for recombination experiments, or minutes for redox titrations), where relaxation phenomena, proton equilibria in particular, may be expected to be completed. It is possible, however, that some very slow relaxation process (> 1 s) is responsible for the discrepancy. The multiphasic character of the decay may actually be taken as a hint for such a process.

The redox titration data for the E_m of Q_A found in the literature are rather scattered. Roughly, three ranges of values were reported, around -250, 0, and 125 mV (reviewed in ref *45*). The -30 mV figure featured in Table 1 is taken from the work of the Rutherford group (for titrations run in the presence of DCMU) (*37*, *44*, *45*) and appears as the most reliable one, owing to a systematic evaluation of critical parameters: effects of mediators, inhibitors, donor side integrity. The authors found little pH dependence of the E_m, at variance with the case of bacterial chromatophores. The low titration wave around -250 mV remains mysterious (see e.g., refs *56*–*58*) but appears unlikely to reflect the Q_A/Q_A^- couple proper, since it was not observed when titrating the C-550 change (*57*). An additional reason for rejecting values in the -300 mV region as reported by Thielen and van Gorkom (*59*) is that this would lead to unacceptably low values for the midpoint potentials of the donor side cofactors,

as explained below. It may also be argued that in algae in vivo under anaerobic conditions, the redox poise is such that Q_A is reduced in the dark (*60*), while in the b_6f complex, heme b_h is entirely reduced and b_l remains mostly oxidized (*61*). This confirms that the midpoint potential of Q_A is significantly more positive than that of b_l (≈ -150 mV (*62*)). As to the high potential wave appearing in some Q_A titrations Krieger and co-workers proposed that it results from the disassembly of the Mn-cluster caused by its reduction when poising PS II at low redox potentials in the presence of redox mediators. The disruption of the Mn cluster induces a $+150$ mV shift of the E_m of Q_A, and this has been proposed to account for the titration wave around $+125$ mV and to be a major source for the scatter of the reported values (*44*, *45*).

Although we cannot rule out the possibility that the "operating potential" of Q_A could be more negative on the time scale of recombination (seconds) than that appearing in redox titrations (minutes), we consider as more likely that the discrepancy arises from the estimation of E_m (Ph), as previously proposed in ref *44*. Indeed, the very negative value of E_m(Ph) renders its determination delicate. The titrations must be performed at low pH (pH 10–11) to prevent hydrogen formation (*63*, *64*). In these experiments, the amount of oxidized Ph was assayed by measuring the amount of Ph^- that can be photoaccumulated under prolonged continuous illumination. Such harsh conditions may affect the protein properties. The estimates obtained in this manner in *R. viridis* range from -400 to -600 mV (*5*, *65*–*67*) and from -600 to -650 mV in PSII (*63*, *64*). Besides the problem of the reliability of the redox titrations, one should consider electrostatic interactions that may have significance with regard to the present issue. A first effect is the interaction between Ph and the anionic Q_A^- expected to be present at the low potential poise where Ph titrates in. Recently, Gibasiewicz et al. (*68*) estimated this interaction at about 90 mV. Thus, the measured E_m of Ph would be 90 mV lower than the true value (unless Q_A was in a neutral reduced form such as Q_AH_2 in these experiments). A second effect is the interaction between P^+ and Ph^-, that will cause a stabilization of the P^+Ph^- state. The center-to-center distance is about 16 Å (assuming the cation is predominantly located on the D1 member of the special pair, see ref *69*) and the expected Coulombic interaction is thus in the range 45–225 mV ($\epsilon_r = 20$–4, respectively). From electrostatic calculations based on the structure of the bacterial reaction center, Parson et al. estimated the interaction between P^+ and BPh_L^- to be about 160 meV (4 kcal/mol) (*70*). This is precisely what would be needed, in addition to the 90 meV interaction of Q_A^- and Ph to obtain a 250 meV shift. It should be noted that these effects have a different status: the first one means that the titrated E_m (Ph) is artifactually offset with respect to the "true" value because of the interaction with Q_A^-, whereas the second one implies that the operational E_m (Ph), regarding the exciton/radical pair equilibrium or the population of the radical pair from a more stabilized state, is more positive than the "true" E_m because of the interaction with P^+.

The issues discussed here for PS II have been the object of a number of studies in the bacterial reaction center (*2*, *5*, *7*). The indirect recombination route through BPh is predominant in *R. viridis* (where Q_A is a menaquinone with lower E_m than ubiquinone), or in modified centers from *R.*
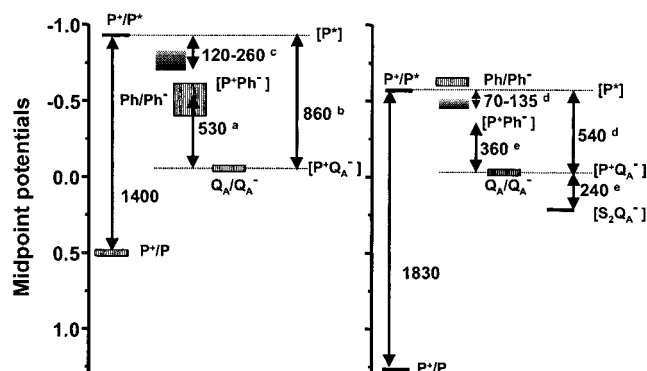
FIGURE 5: Energetics of the excited and radical pair states in *R. sphaeroides* (left) and photosystem II (right). The redox couples are positioned with respect to the midpoint potentials scale (in V). The relative energy levels of charge-separated states (indicated between brackets) are plotted with respect to the E_m of Q_A. The gray boxes indicate the range of midpoints potentials obtained in equilibrium redox titrations. For Ph/Ph$^-$, no data are available for *R. sphaeroides*, and we used results from *R. viridis* (*5, 65−67*). The PS II titrations of Ph/Ph$^-$ are from refs *63* and *64*. The levels indicated with solid lines are midpoints potentials deduced from free energy changes (the latter indicated by arrows, values expressed in meV). The time-dependent relaxation between P* and P$^+$Ph$^-$ is symbolized by shaded boxes [c: (*72, 83*) for *sphaeroides* and d: (*50, 81*) for PS II]. The free energy difference between P$^+$Ph$^-$ and P$^+$Q$_A$$^-$ in *R. sphaeroides* has been determined from its estimation in anthraquinone-substituted reaction centers (370 meV) and the difference in midpoint potentials between anthraquinone and ubiquinone (160 mV) (a: *83*). The free energy change between P* and P$^+$Q$_A$$^-$ was taken from (b: *74*) for *R. sphaeroides* and derived from the luminescence yield (d: *14*) for PS II. Other values are determined in this paper (e).

sphaeroides with a reduced free energy gap between BPh and Q_A (e.g., by substituting anthraquinones for Q_A (*2, 7, 71*). In such cases, the recombination rates lead to estimates of the ΔG between quinone and BPh (e.g., about 370 meV in anthraquinone substituted centers) which are markedly smaller than those derived from the exciton−radical pair equilibrium as measured in the subnanosecond range, suggesting that the P$^+$BPh$^-$ state undergoes substantial stabilization at later times (*7*). This view is supported by luminescence studies showing evidence of relaxation phases occurring on a broad range of time scales (*72*). The E_m of BPh obtained by redox titration (thus, obviously, under "relaxed" conditions) is about −620 mV (*67, 73*), corresponding to G_{QBPh} ≈ 620−210 = 410 meV (where −210 mV is the E_m of the anthraquinone). This is larger by 40 meV than the value required to match the recombination data, but the discrepancy is clearly not as big as in PS II. A comparison between the E_m data in bacteria and PS II is shown in Figure 5 to highlight the point made in this paper. Roughly similar values have been found for (B)Ph and Q_A (in reaction centers with UQ, as *R. sphaeroides*), while the recombination route is direct in bacteria and predominantly indirect in PS II. Also, the luminescence yields differ by many orders of magnitude. Indeed, according to the data of Arata and Parson (*74*), the absolute value of the radiative contribution to the excitonic pathway in *R. sphaeroides* is about 2 × 10^{-8}. Such a low value clearly implies that the relative weight of the total excitonic pathway in the recombination process is much smaller than in PSII (3%, *14*). Altogether, this points to an erroneous E_m picture in PS II. A point that remains unclear, however, is why the discrepancy that we ascribe to the E_m

of (B)Ph is only about 60 mV in bacteria versus 250 mV in PS II. The (≈ 90 meV) interaction between $Q_A$$^-$ and Ph that was proposed to affect the redox titration of Ph may not occur in bacteria if the binding of one proton (as suggested by the pH dependence of the E_m of Q_A in chromatophores) cancels the effect. The other contribution (≈160 meV) ascribed to the electrostatic interaction between P$^+$ and (B)Ph$^-$ should however be present.

On the basis of de Grooth's estimate for the excitonic recombination yield, we have estimated the free energy difference between P*Q_A and S_2P$Q_A$$^-$ to be around 780 meV. Thus, if G_{SP} = 240 meV, the free energy difference between P*Q_A and P$^+$Q$_A$$^-$ is 540 meV. Then, if we accept E_m (Q_A) ≈ −30 mV as a reliable value for the "operating potential" of Q_A during recombination (i.e., if we consider that no significant relaxation occurs on a longer time-scale than the seconds time-range, see above), this has significant consequences on the estimation of the E_m of the donor side cofactors. Indeed, the midpoint potentials of (P$^+$/P*), (P$^+$/P), (Y$_Z^{ox}$/Y$_Z$) and those of the S states have not been measured directly, but located primarily with respect to (Ph/Ph$^-$). First, one obtains E_m (P$^+$/P*) ≈ −540 − 30 = −570 mV (assuming that the interaction between P$^+$ and $Q_A$$^-$ is negligible). This is 150 mV higher than the −720 mV figure quoted in Table 1 (the offset is smaller than the above estimate of 250 mV because the estimation featured in Table 1 did not take into account the entropic stabilization of the exciton on the antenna). Then, one has E_m(P$^+$/P) ≈ 1830 − 570 = +1260 mV (taking 1830 mV as the energy of the singlet−singlet transition on P, see Figure 5), again 150 mV higher than in Table 1. Furthermore, E_m(S_2/S_1) ≈ 1260 − 240 = 1020 mV. This implies that the driving force for water oxidation is significantly larger than previously estimated and it would then be less of an amazing feat (see, e.g., refs *1, 75, 76−78*) to ensure the efficiency of this complex reaction (the midpoint potential of the O_2/H_2O couple is + 930 mV at pH 5, which is likely close to the physiological pH of the lumen). Conversely, if one had chosen the alternative option assuming that the titration value of Ph is correct and that the midpoint potential of Q_A is 250 mV lower than −30 mV, one would obtain E_m(P$^+$/P) ≈ 1010 mV and E_m(S_2/S_1) ≈ 770 mV. This would make water oxidation impossible unless the higher states have E_m's close to 1000 mV, in which case only 10 mV would be available to drive the oxidation of S_2 and S_3 by P$^+$.

ACKNOWLEDGMENT

REFERENCES

1. Diner, B. A., and Babcock, G. T. (1996) in *Oxygenic Photosynthesis: The Light Reactions* (Ort, D. R., and Yocum, C. F., Eds.) pp 213−247, Kluwer Academic Publishers, Dordrecht.
2. Gunner, M. R., Liang, Y., Nagus, D. K., Hochstrasser, R. M., and Dutton, P. L. (1982) *Biophys. J. 37*, 226.
3. Baciou, L., Bylina, E. J., and Sebban, P. (1993) *Biophys. J. 65*, 652−660.
4. Miksovska, J., Maroti, P., Tandori, J., Schiffer, M., Hanson, D. K., and Sebban, P. (1996) *Biochemistry 35*, 15411−15417.
5. Shopes, R. J., and Wraight, C. A. (1987) *Biochim. Biophys. Acta 893*, 409−425.

6. Parson, W. W. (1996) in *Protein Electron Transfer* (Bendall, D. S., Ed.) pp 125−160, BIOS Scientific Publishers Ltd, Oxford.

7. Woodbury, N. W., Parson, W. W., Gunner, M. R., Prince, R. C., and Dutton, P. L. (1986) *Biochim. Biophys. Acta 851*, 6−22.

8. van Gorkom, H. J. (1985) *Photosynth. Res. 6*, 97−112.

9. Reinman, S., and Mathis, P. (1981) *Biochim. Biophys. Acta 635*, 249−258.

10. Vavilin, D. V., and Vermaas, W. F. (2000) *Biochemistry 39*, 14831−14838.

11. Bernarding, J., Eckert, H.-J., Eichler, H.-J., Napiwotzki, A., and Renger, G. (1994) *Photochem. Photobiol. 59*, 566−573.

12. Nuijs, A. M., van Gorkom, H. J., Plijter, J. J., and Duysens, L. N. M. (1986) *Biochim. Biophys. Acta 848*, 167−175.

13. Trissl, H.-W., and Leibl, W. (1989) *FEBS Lett. 244*, 85−88.

14. De Grooth, B. G., and van Gorkom, H. J. (1981) *Biochim. Biophys. Acta 635*, 445−456.

15. Ide, J. P., Klug, D. R., Kühlbrandt, W., Giorgi, L. B., and Porter, G. (1987) *Biochim. Biophys. Acta 893*, 349−364.

16. Nordlund, T. M., and Knox, W. H. (1981) *Biophys. J. 36*, 193−201.

17. Giorgi, L. B., Nixon, P. J., Merry, S. A. P., Joseph, D. M., Durrant, J. R., Rivas, J. D., Barber, J., Porter, G., and Klug, D. R. (1996) *J. Biol. Chem. 271*, 2093-2101.

18. Merry, S. A. P., Nixon, P. J., Barter, L. M. C., Schilstra, M. J., Porter, G., Barber, J., Durrant, J. R., and Klug, D. (1998) *Biochemistry 37*, 17439−17447.

19. Dorlet, P., Xiong, L., Sayre, R. T., and Un, S. (2001) *J. Biol. Chem. 276*, 22313−22316.

20. Allen, J. P., and Williams, J. C. (1995) *J. Bioenerg. Biomembr. 27*, 275−283.

21. Williams, J. G. K. (1988) *Methods Enzymol. 167*, 766−778.

22. Nixon, P. J., Trost, J. T., and Diner, B. A. (1992) *Biochemistry 31*, 10859−10871.

23. Joliot, P., Béal, D., and Frilley, B. (1980) *J. Chim. Phys. 77*, 209−216.

24. Joliot, P., Joliot, A., and Verméglio, A. (1997) *Biochim. Biophys. Acta 1318*, 374−384.

25. Joliot, P., and Joliot, A. (1964) *C. R. Acad. Sci. Paris 258*, 4622−4625.

26. Paillotin, G. (1976) *J. Theor. Biol. 58*, 237−252.

27. Diner, B. A., and Wollman, F.-A. (1979) *Plant Physiol. 63*, 20−25.

28. Bennoun, P. (1970) *Biochim. Biophys. Acta 216*, 357−363.

29. Conjeaud, H., and Mathis, P. (1980) *Biochim. Biophys. Acta 590*, 353−359.

30. Hillmann, B., and Schlodder, E. (1995) *Biochim. Biophys. Acta 1231*, 76−88.

31. Moënne-Loccoz, P., Robert, B., and Lutz, M. (1989) *Biochemistry 28*, 3641−3645.

32. Diner, B. A., Nixon, P. J., and Farchaus, J. W. (1991) *Curr. Opin. Struct. Biol. 1*, 546−554.

33. Svensson, B., Etchebest, C., Tuffery, P., van Kan, P., Smith, J., and Styring, S. (1996) *Biochemistry 35*, 14486-14502.

34. Ruffle, S. V., Donnelly, D., Blundell, T. L., and Nugent, J. H. A. (1992) *Photosynth. Res. 34*, 287−300.

35. Breton, J., Bibikova, M., Oesterhelt, D., and Nabedryk, E. (1999) *Biochemistry 38*, 11541−11552.

36. Breton, J., Nabedryk, E., Allen, J. P., and Williams, J. A. C. (1997) *Biochemistry 36*, 4515−4525.

37. Krieger-Liszkay, A., and Rutherford, A. W. (1998) *Biochemistry 37*, 17339−17344.

38. Brettel, K., Schlodder, E., and Witt, H. T. (1984) *Biochim. Biophys. Acta 766*, 403−415.

39. Eckert, H.-J., and Renger, G. (1988) *FEBS Lett. 236*, 425−431.

40. Rappaport, F., Porter, G., Barber, J., Klug, D., and Lavergne, J. (1995) in *Photosynthesis: From Light to Biosphere* (Mathis, P., Ed.) pp 345−348, Kluwer Academic Publishers, Dordrecht.

41. Vos, M. H., van Gorkom, H. J., and van Leeuwen, P. J. (1991) *Biochim. Biophys. Acta 1056*, 27−39.

42. Gerken, S., Dekker, J. P., Schlodder, E., and Witt, H. T. (1989) *Biochim. Biophys. Acta 977*, 52−61.

43. Metz, J. G., Nixon, P. J., Rögner, M., Brudvig, G. W., and Diner, B. A. (1989) *Biochemistry 28*, 6960−6969.

44. Johnson, G. N., Rutherford, A. W., and Krieger, A. (1995) *Biochim. Biophys. Acta 1229*, 202−207.

45. Krieger, A., Rutherford, A. W., and Johnson, G. N. (1995) *Biochim. Biophys. Acta 1229*, 193−201.

46. Moser, C. C., Page, C. C., Farid, R., and Dutton, P. L. (1995) *J. Bioenerg. Biomembr. 27*, 263−274.

47. Haberkorn, R., and Michel-Beyerle, M. E. (1979) *Biophys. J. 26*, 489−498.

48. Volk, M., Gilbert, M., Rousseau, G., Richter, M., Ogrodnik, A., and Michel-Beyerle, M. E. (1993) *FEBS Lett. 336*, 357−362.

49. van Mieghem, F. J. E., Brettel, K., Hillmann, B., Kamlowski, A., Rutherford, A. W., and Schlodder, E. (1995) *Biochemistry 34*, 4798−4813.

50. Booth, P. J., Crystall, B., Ahmad, I., Barber, J., Porter, G., and Klug, D. R. (1991) *Biochemistry 30*, 7573−7586.

51. Zouni, A., Witt, H. T., Kern, J., Fromme, P., Krauss, N., Saenger, W., and Orth, P. (2001) *Nature 409*, 739−743.

52. Vass, I., Horvath, G., Herczeg, T., and Demeter, S. (1981) *Biochim. Biophys. Acta 634*, 140−152.

53. Randall, J. F., and Wilkins, J. H. F. (1945) *Proc. Royal Soc. 184*, 389.

54. Devault, D., Govindjee, and Arnold, W. (1983) *Proc. Natl. Acad. Sci. U.S.A. 80*, 983−987.

55. van Gorkom, H. J., Meiburg, R. F., and De Vos, L. J. (1986) *Photosynth. Res. 9*, 55−62.

56. Cramer, W. A., and Butler, W. L. (1969) *Biochim. Biophys. Acta 172*, 503−510.

57. Diner, B. A., and Delosme, R. (1983) *Biochim. Biophys. Acta 722*, 443−451.

58. Evans, M. C. W., Atkinson, Y. E., and Ford, R. C. (1985) *Biochim. Biophys. Acta 806*, 247−254.

59. Thielen, A. P. G. M., and van Gorkom, H. J. (1981) *FEBS Lett. 129*, 205−209.

60. Diner, B. A. (1977) *Biochim. Biophys. Acta 460*, 247−258.

61. Joliot, P., and Joliot, A. (1994) *Proc. Natl. Acad. Sci. U.S.A. 91*, 1034−1038.

62. Pierre, Y., Breyton, C., Kramer, D., and Popot, J.-L. (1995) *J. Biol. Chem. 49*, 29342−29349.

63. Klimov, V. V., Allakhverdiev, S. I., Demeter, S., and Krasnovskii, A. A. (1979) *Dokl. Akad. Nauk SSSR 249*, 227−230.

64. Rutherford, A. W., Mullet, J. E., and Crofts, A. R. (1981) *FEBS Lett. 123*, 235−237.

65. Prince, R. C., Leigh, J. S., and Dutton, P. L. (1976) *Biochim. Biophys. Acta 440*, 622−636.

66. Shuvalov, V. A., Krakhmaleva, I. N., and Klimov, V. V. (1976) *Biochim. Biophys. Acta 449*, 597−601.

67. Rutherford, A. W., Heathcote, P., and Evans, M. C. W. (1979) *Biochem. J. 182*, 523.

68. Gibasiewicz, K., Dobek, A., Breton, J., and Leibl, W. (2001) *Biophys. J. 80*, 1617−1630.

69. Diner, B. A., Schlodder, E., Nixon, P. J., Coleman, W. J., Rappaport, F., Lavergne, J., Vermaas, W. F., and Chisholm, D. A. (2001) *Biochemistry 40*, 9265−9281.

70. Parson, W. W., Chu, Z.-T., and Warshel, A. (1990) *Biochim. Biophys. Acta 1017*, 251−272.

71. Sebban, P. (1988) *FEBS Lett. 233*, 331−334.

72. Peloquin, J. M., Williams, J. C., Lin, X. M., Alden, R. G., Taguchi, A. K. W., Allen, J. P., and Woodbury, N. W. (1994) *Biochemistry 33*, 8089−8100.

73. Shopes, R. J., and Wraight, C. A. (1986) *Biochim. Biophys. Acta 848*, 364−371.

74. Arata, H., and Parson, W. W. (1981) *Biochim. Biophys. Acta 638*, 201−209.

75. Haumann, M., and Junge, W. (1996) in *Oxygenic Photosynthesis: The Light Reaction* (Ort, D. R., and Yocum, C. F., Eds.) pp 165−192, Kluwer Acad., Dordrecht.

76. Rappaport, F., and Lavergne, J. (2001) *Biochim. Biophys. Acta 1503*, 246−259.

77. Renger, G. (2001) *Biochim. Biophys. Acta 1503*, 210−228.

78. Tommos, C., and Babcock, G. T. (2000) *Biochim. Biophys. Acta 1458*, 199−219.

79. Klimov, V. V., Allakhverdiev, S. I., and Pashchenko, V. Z. (1978) *Dokl. Akad. Nauk. SSSR 242*, 1204−1207.

80. Holzwarth, A. R. (1986) *Photochem. Photobiol. 43*, 707−725.

81. Booth, P. J., Crystall, B., Giorgi, L. B., Barber, J., Klug, D. R., and Porter, G. (1990) *Biochim. Biophys. Acta 1016*, 141−152.

82. Roelofs, T. A., Gilbert, M., Shuvalov, V. A., and Holzwarth, A. R. (1991) *Biochim. Biophys. Acta 1060*, 237−244.

83. Woodbury, N. W., and Parson, W. W. (1986) *Biochim. Biophys. Acta 850*, 197−210.